Electronic Supplementary Material (ESI) for Sustainable Energy & Fuels.
This journal is © The Royal Society of Chemistry 2020

Supporting information

for

Synergetic FeCo nanorods embedded in nitrogen doped carbon nanotubes with abundant metal-NCNT heterointerfaces as efficient air electrocatalyst for rechargeable zinc-air batteries

Hao Hu[a#], Yuhua Xie[a#], Farhad MD Kazim[a], Konggang Qu[b], Min Li[a], Zhikun Xu[c,d*] and Zehui Yang[a*]

[a]Sustainable Energy Laboratory, Faculty of Materials Science and Chemistry, China University of Geosciences Wuhan, 388 Lumo RD, Wuhan, 430074, China

[b]Shandong Provincial Key Laboratory/Collaborative Innovation Center of Chemical Energy Storage & Novel Cell Technology, Liaocheng University, Liaocheng, 252059, China

[c]Key Laboratory for Photonic and Electronic Bandgap Materials, Ministry of Education, School of Physics and Electronic Engineering, Harbin Normal University, Harbin 150025, China.

[d]College of Science, Guangdong University of Petrochemical Technology,, Maoming, 525000, China.

H. Hu and Y. Xie equally contributed to this work.

Table S1 Quantitative analysis of N1s peaks of various electrocatalysts.

Electrocatalyst	pyridinic N	pyrollic N	graphitic N	oxidized N
Fe-NR/NCNT	30.72	21.60	29.76	17.92
Co-NR/NCNT	28.31	21.51	29.02	21.16
$Fe_{0.67}Co_{0.33}$-NR/NCNT	30.33	22.24	28.08	19.35
$Fe_{0.5}Co_{0.5}$-NR/NCNT	31.72	22.15	31.61	18.52
$Fe_{0.33}Co_{0.67}$-NR/NCNT	34.49	23.57	30.38	11.56

Table S2 Quantitative analysis of Fe2p and Co2p peaks of various electrocatalysts.

Electrocatalyst	Fe^0:Fe^{x+}	Co^0:Co^{x+}
Fe-NR/NCNT	1.98:1	-
Co-NR/NCNT	-	4.17:1
$Fe_{0.67}Co_{0.33}$-NR/NCNT	1.76:1	1.92:1
$Fe_{0.5}Co_{0.5}$-NR/NCNT	1.79:1	1.90:1
$Fe_{0.33}Co_{0.67}$-NR/NCNT	1.82:1	1.83:1

Table S3 Comparison of power densities of rechargeable zinc-air batteries based on Fe/Co electrocatalysts.

Electrocatalyst	Power density (mW cm^{-2})	Ref.
$Fe_{0.5}Co_{0.5}$-NR/NCNT	164	This work
FeCo-Nx-CN	150	[1]
CoFe@NCNTs	150	[2]
Co_2FeO_4/NCNTs	90.68	[3]
CoFe/N-GCT	203	[4]
FeNi@N-CNT/NCSs	103	[5]
D-BNGFe	142	[6]
Mn/Co-N-C	136	[7]
CoFe/Co@NCNT/NG	161	[8]
Co–N–C nanosheet	132	[9]

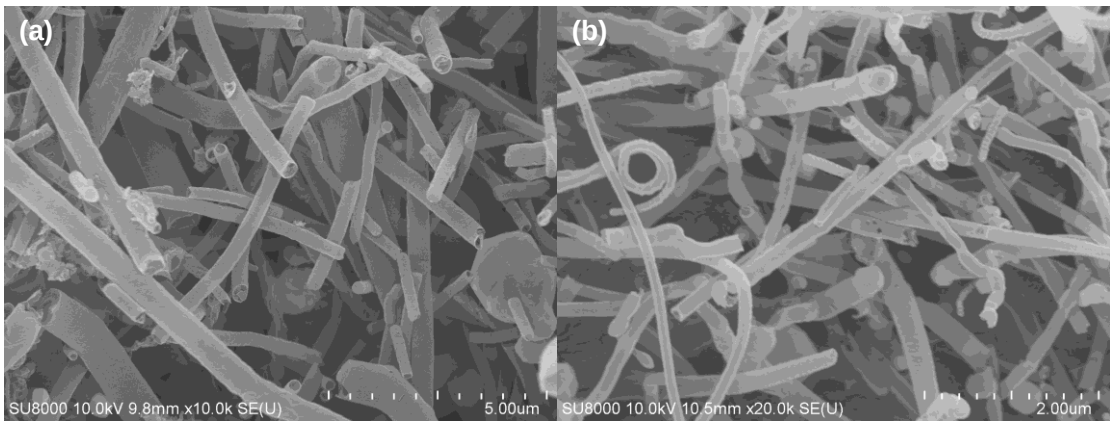

Figure S1 SEM images of $Fe_{0.67}Co_{0.33}$-NR/NCNT (a) and $Fe_{0.5}Co_{0.5}$-NR/NCNT (b) electrocatalysts.

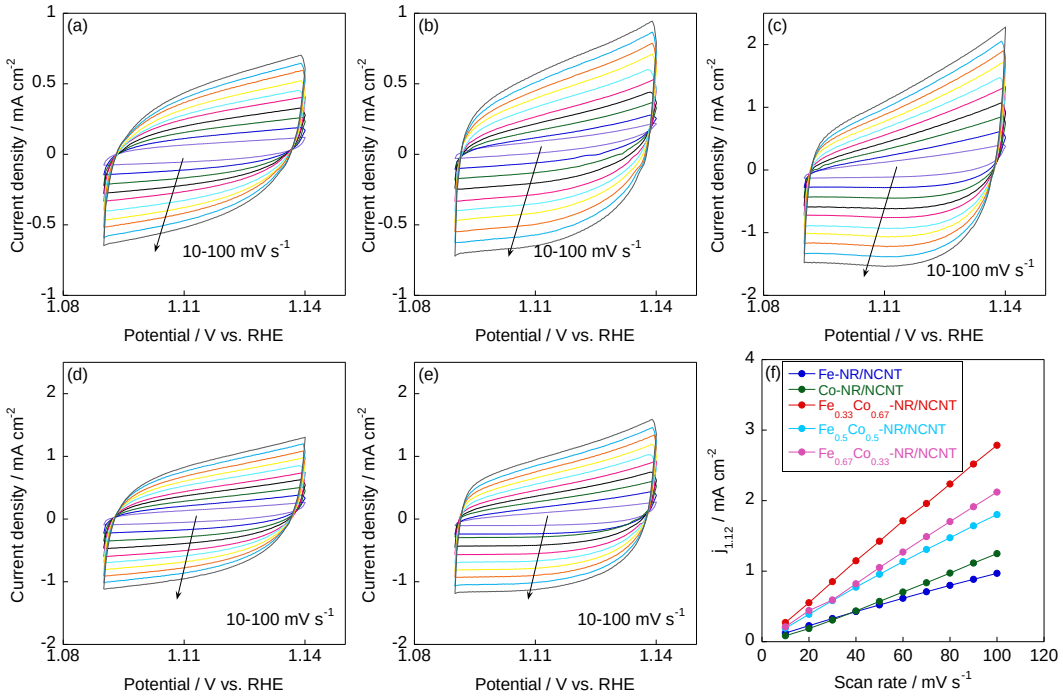

Figure S2 Cyclic voltammetry curves of Fe-NR/NCNT (a), Co-NR/NCNT (b), $Fe_{0.33}Co_{0.67}$-NR/NCNT (c), $Fe_{0.5}Co_{0.5}$-NR/NCNT (d) and $Fe_{0.67}Co_{0.33}$-NR/NCNT (e) electrocatalysts. (f) ECSAs of Fe-NR/NCNT, Co-NR/NCNT, $Fe_{0.67}Co_{0.33}$-NR/NCNT, $Fe_{0.5}Co_{0.5}$-NR/NCNT and $Fe_{0.33}Co_{0.67}$-NR/NCNT electrocatalysts.

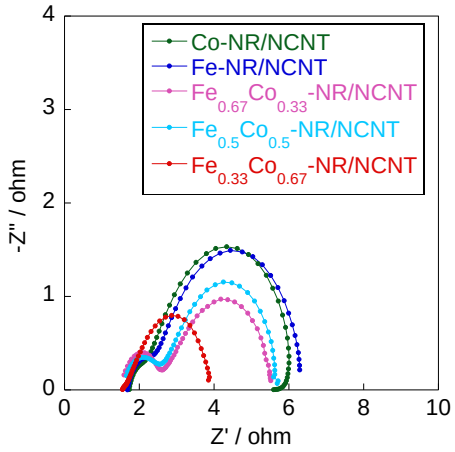

Figure S3 Electrochemical impedance spectroscopies (EIS) of Fe-NR/NCNT, Co-NR/NCNT, $Fe_{0.67}Co_{0.33}$-NR/NCNT, $Fe_{0.5}Co_{0.5}$-NR/NCNT and Fe0.33Co0.67-NR/NCNT electrocatalysts.

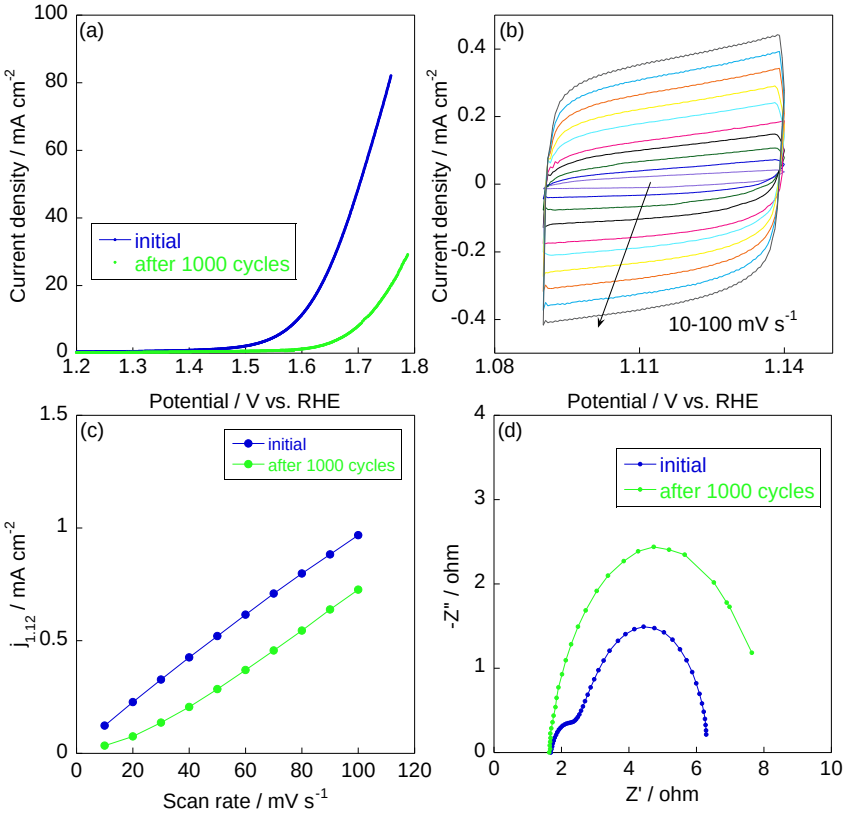

Figure S4 OER performance (a), cyclic voltammetry curve (b), ECSA (c) and electrochemical impedance spectroscopies (d) of Fe-NR/NCNT before and after 1000 potential cycles.

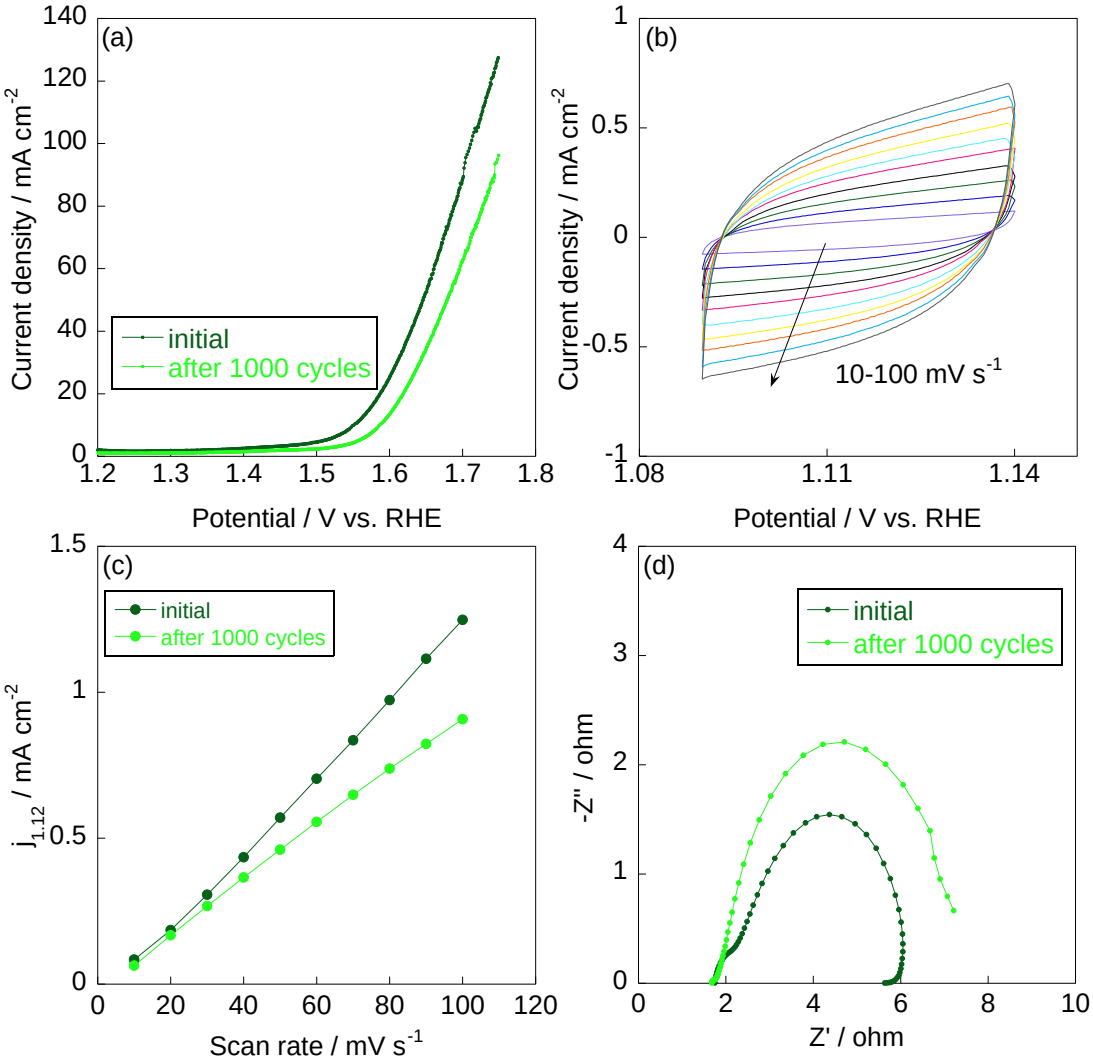

Figure S5 OER performance (a), cyclic voltammetry curve (b), ECSA (c) and electrochemical impedance spectroscopies (d) of Co-NR/NCNT before and after 1000 potential cycles.

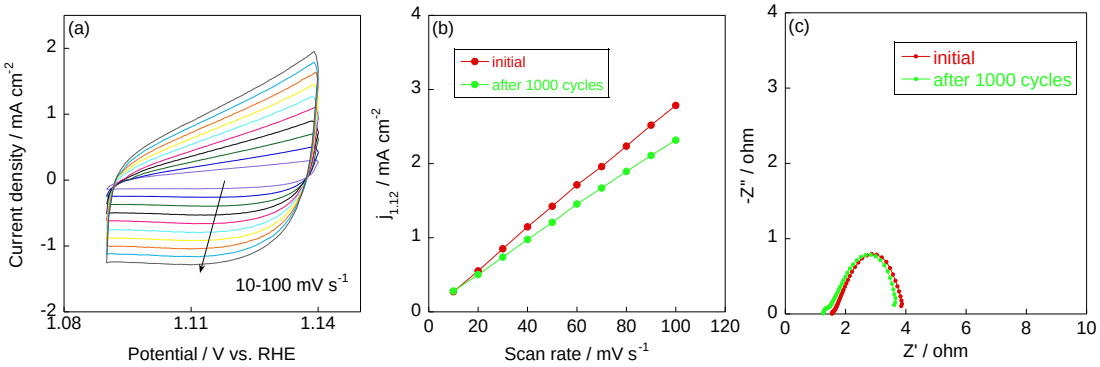

Figure S6 Cyclic voltammetry curve (a), ECSA (b) and electrochemical impedance spectroscopies (c) of $Fe_{0.33}Co_{0.67}$-NR/NCNT before and after 1000 potential cycles.

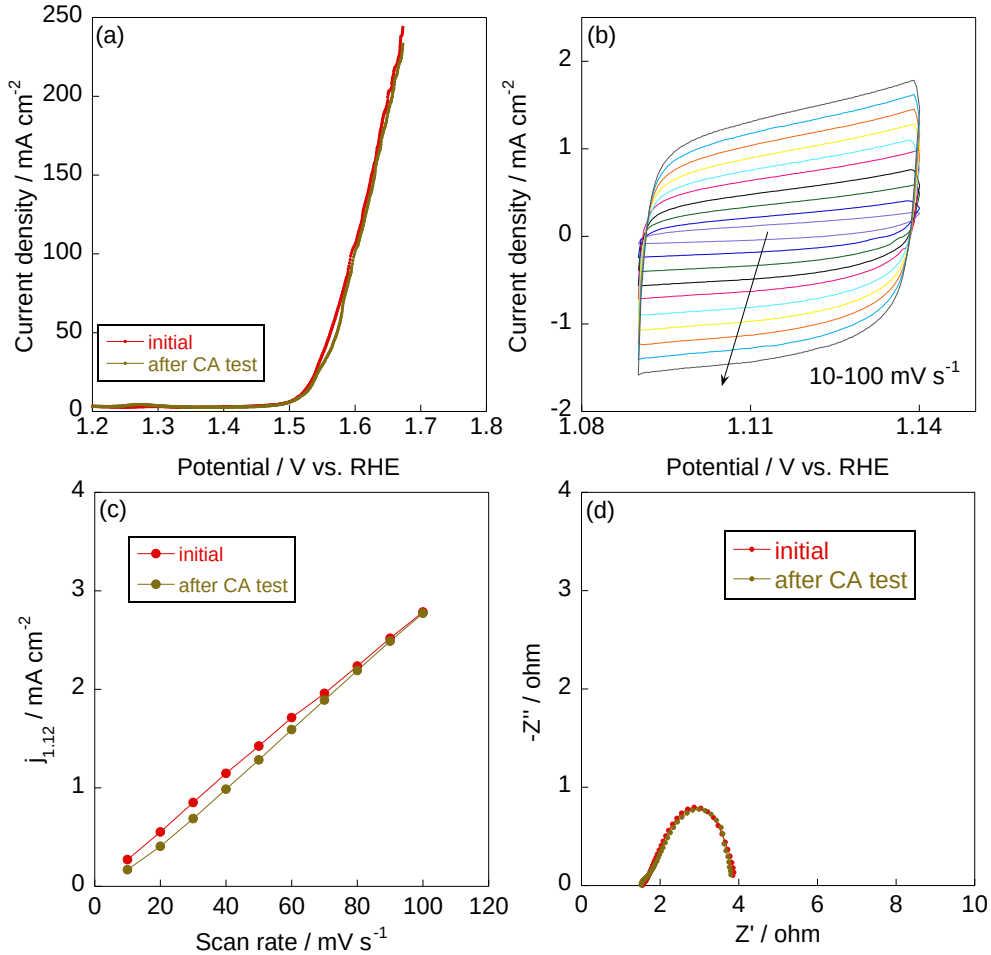

Figure S7 OER performance (a), cyclic voltammetry curve (b), ECSA (c) and electrochemical impedance spectroscopies (d) of $Fe_{0.33}Co_{0.67}$-NR/NCNT before and after 1000 potential cycles.

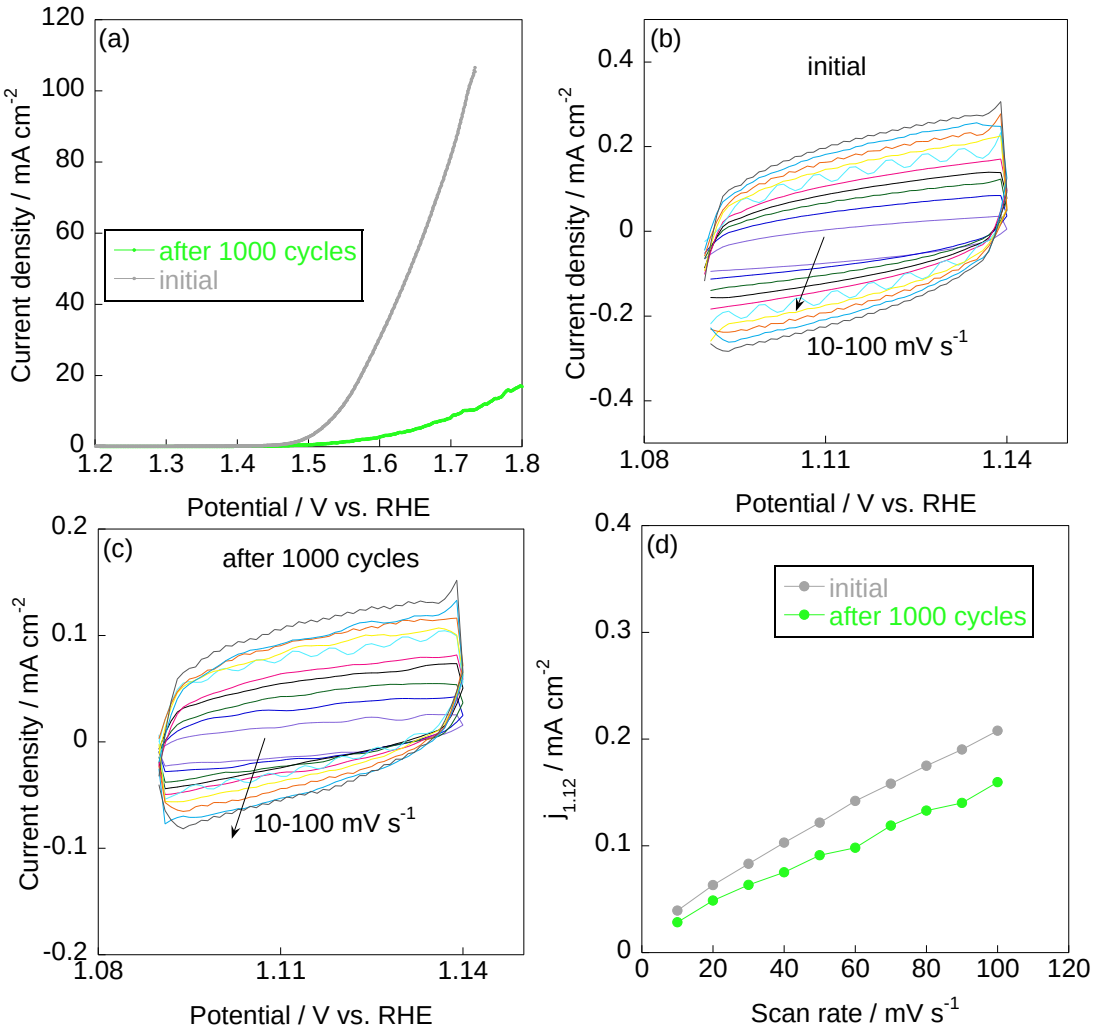

Figure S8 OER performance (a), cyclic voltammetry curves (b, c) and ECSAs (d) of commercial IrO_2 before and after 1000 potential cycles.

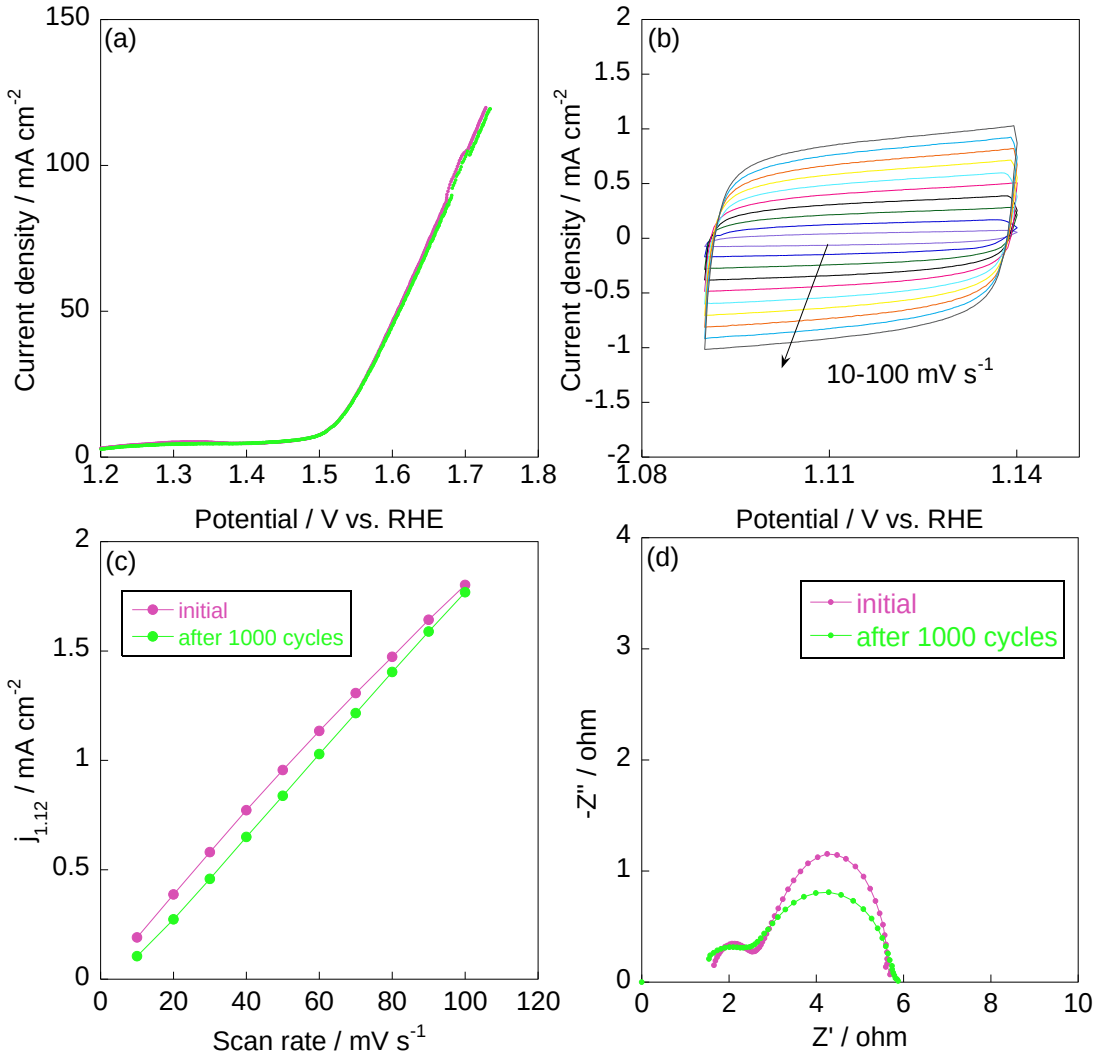

Figure S9 OER performance (a), cyclic voltammetry curve (b), ECSA (c) and electrochemical impedance spectroscopies (d) of $Fe_{0.5}Co_{0.5}$-NR/NCNT before and after 1000 potential cycles.

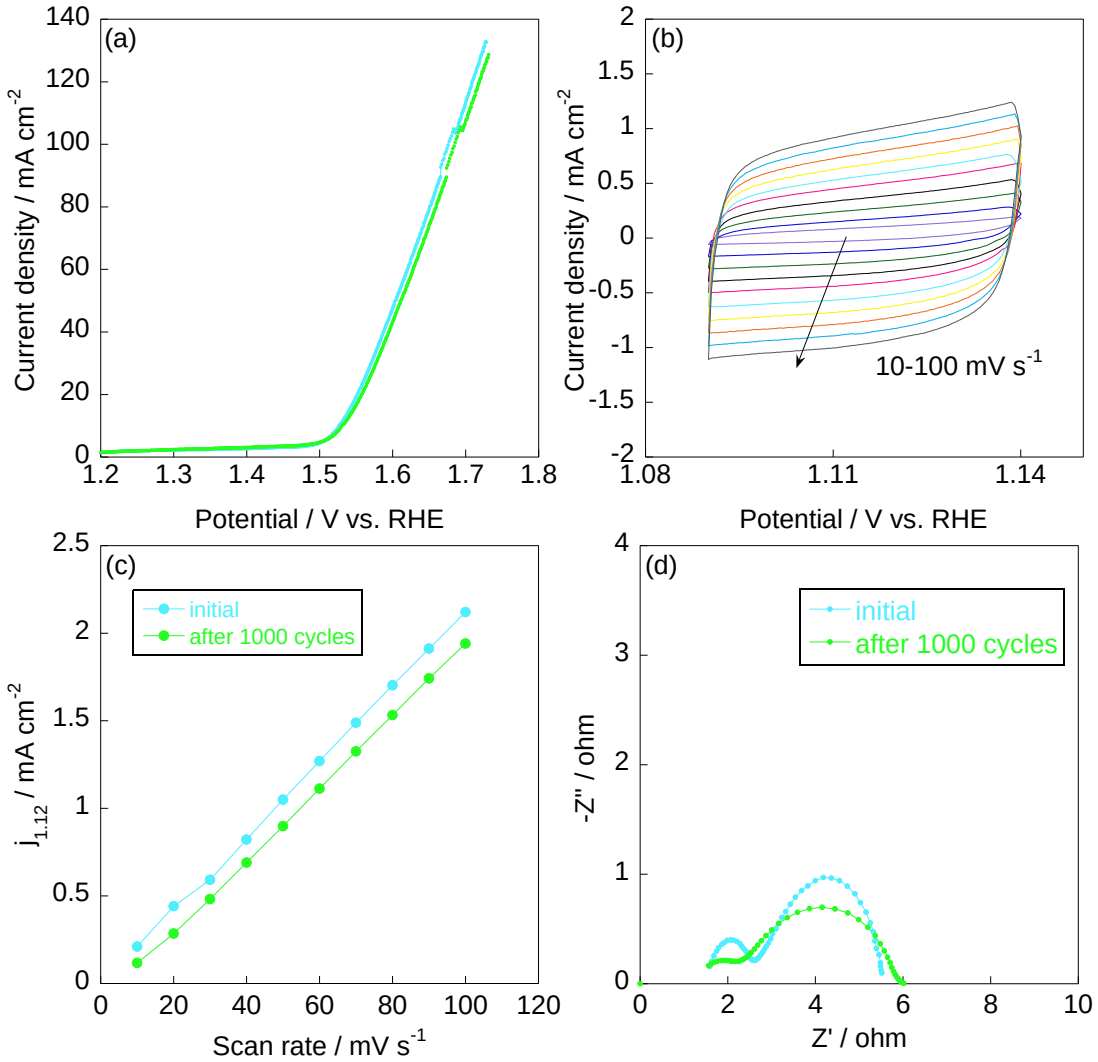

Figure S10 OER performance (a), cyclic voltammetry curve (b), ECSA (c) and electrochemical impedance spectroscopies (d) of $Fe_{0.67}Co_{0.33}$-NR/NCNT before and after 1000 potential cycles.

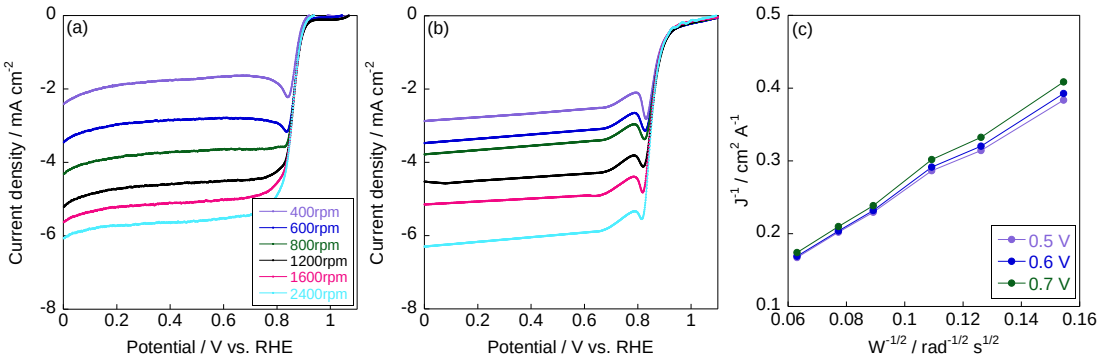

Figure S11 LSV curves of $Fe_{0.33}Co_{0.67}$-NR/NCNT (a) and commercial Pt/C (b) electrocatalysts with various scan speeds. (c) Number of transferred electrons at various potentials for commercial Pt/C electrocatalyst.

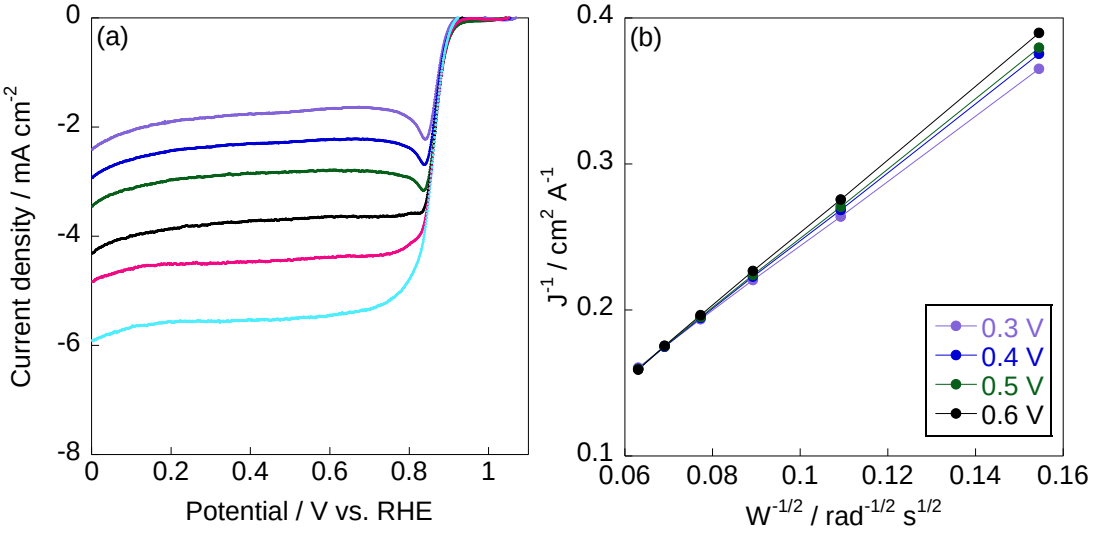

Figure S12 (a) LSV curves of $Fe_{0.33}Co_{0.67}$-NR/NCNT electrocatalyst with various scan speeds after 1000 potential cycles. (b) Number of transferred electrons at various potentials for $Fe_{0.33}Co_{0.67}$-NR/NCNT electrocatalyst.

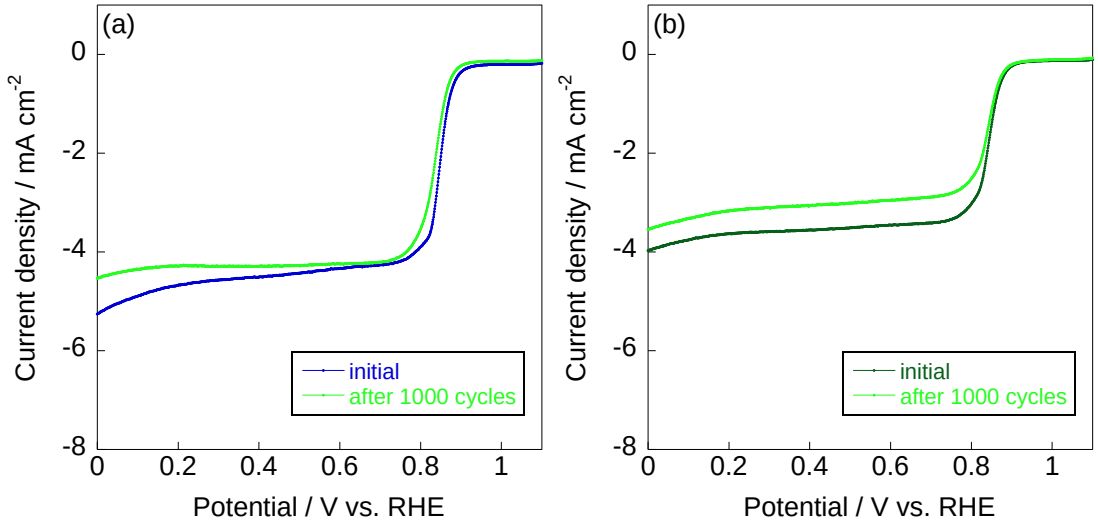

Figure S13 ORR curves of Fe-NR/NCNT (a) and Co-NR/NCNT electrocatalysts before and after 1000 potential cycles.

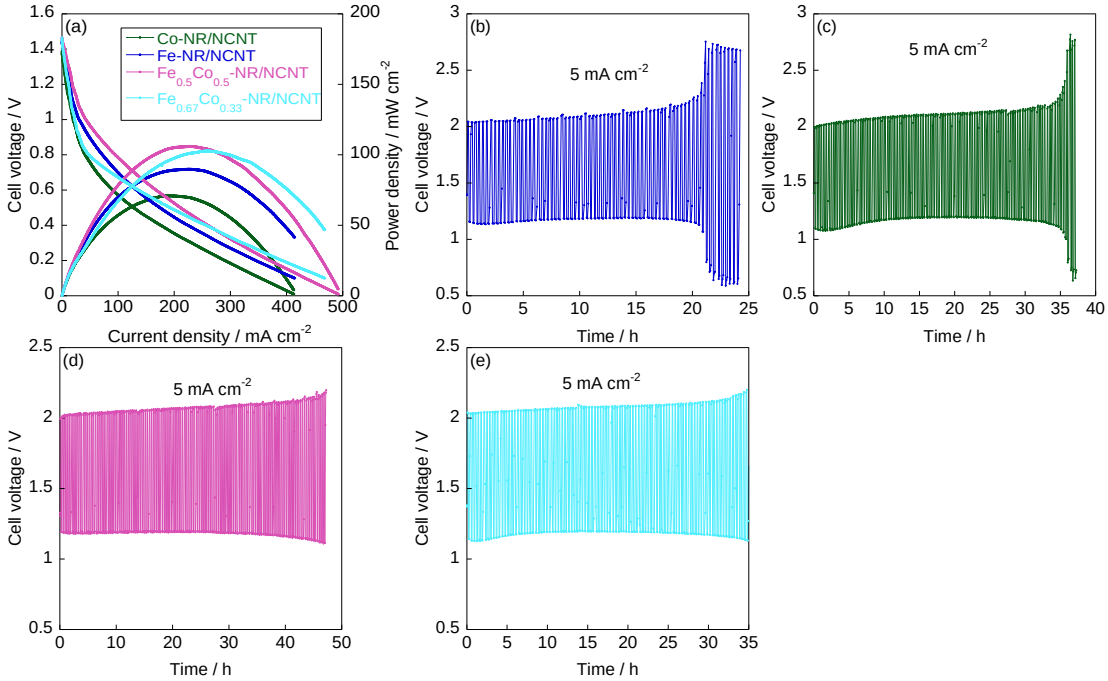

Figure S14 (a) I-V and power density polarization curves of various electrocatalysts. (b) Charge-discharge polarization curves of Fe-NR/NCNT (b), Co-NR/NCNT (c), $Fe_{0.5}Co_{0.5}$-NR/NCNT (d) and $Fe_{0.67}Co_{0.33}$-NR/NCNT (e) electrocatalyst.

References

1. S. Li, C. Cheng, X. Zhao, J. Schmidt and A. Thomas, *Angew. Chem. Int. Ed.*, 2018, **57**, 1856-1862.
2. P. Cai, Y. Hong, S. Ci and Z. Wen, *Nanoscale*, 2016, **8**, 20048-20055.
3. X.-T. Wang, T. Ouyang, L. Wang, J.-H. Zhong, T. Ma and Z.-Q. Liu, *Angew. Chem. Int. Ed.*, 2019, **58**, 13291-13296.
4. X. Liu, L. Wang, P. Yu, C. Tian, F. Sun, J. Ma, W. Li and H. Fu, *Angew. Chem. Int. Ed.*, 2018, **57**, 16166-16170.
5. J.-T. Ren, L. Chen, Y.-S. Wang, W.-W. Tian, L.-J. Gao and Z.-Y. Yuan, *ACS Sustain. Chem. Eng.*, 2020, **8**, 223-237.
6. G. Zhang, X. Liu, L. Wang, F. Sun, Y. Yang, C. Tian, P. Yu, Q. Pan and H. Fu, *ACS Sustain. Chem. Eng.*, 2019, **7**, 19104-19112.
7. L. Wei, L. Qiu, Y. Liu, J. Zhang, D. Yuan and L. Wang, *ACS Sustain. Chem. Eng.*, 2019, **7**, 14180-14188.
8. P. Zhu, J. Gao and S. Liu, *J. Power Sources*, 2020, **449**, 227512.
9. P. Yu, L. Wang, F. Sun, Y. Xie, X. Liu, J. Ma, X. Wang, C. Tian, J. Li and H. Fu, *Adv. Mater.*, 2019, **31**, 1901666.